

NMR investigation of atomic ordering in $\text{Al}_x\text{Ga}_{1-x}\text{As}$ thin films

C. Degen, M. Tomaselli, and B. H. Meier*
Physical Chemistry, ETH Zürich, CH-8093 Zürich, Switzerland

M. M. A. J. Voncken and A. P. M. Kentgens†
NSRIM Center, University of Nijmegen, 6525 ED Nijmegen, The Netherlands
(Received 8 December 2003; published 11 May 2004)

Nuclear magnetic resonance is used to study the local cation ordering in thin films of $\text{Al}_x\text{Ga}_{1-x}\text{As}$ ($0 < x < 0.5$) grown by metal organic vapor phase epitaxy. A quantitative analysis of the ^{75}As resonance intensities and the quadrupole coupling constants of all nuclei reveal that our data is compatible with the absence of significant ordering.

DOI: 10.1103/PhysRevB.69.193303

PACS number(s): 68.55.Jk

Atomic ordering in ternary semiconductor alloys has been shown to be important because of its influence on the material's electronic structure as well as its relation to electronic transport properties, phase transitions, and thermodynamic stability.¹⁻³ The characterization of order in these compounds is crucial in view of a controlled growth of designed semiconductor structures.¹⁻⁴ For $\text{Al}_x\text{Ga}_{1-x}\text{As}$ qualitative information on long-range order with a modulated composition along specific lattice directions has been found.³ The fully ordered structures have been proposed as alternating AlAs and GaAs planes along, e.g., (001) (CuAu-type) or (111) (CuPt-type), respectively [see Figs. 1(b), 1(c)]. A clustering of Al (and Ga) has also been suggested. It is clear that both short- and long-range order affect the local symmetry of the atomic sites in the crystal lattice. In this study we employ nuclear magnetic resonance (NMR) to quantify the degree of atomic ordering in $\text{Al}_x\text{Ga}_{1-x}\text{As}$ ($0 < x < 0.5$) grown by metal organic vapor phase epitaxy (MOVPE) on a (100) GaAs substrate. The results are compatible with the absence of order for the investigated $\text{Al}_x\text{Ga}_{1-x}\text{As}$ thin films.^{2,5}

The samples were grown by MOVPE in a horizontal Aixtron 200 reactor at a growth temperature of 923 K and a rate of $1.8 \mu\text{m/h}$ using trimethyl-gallium and trimethyl-aluminum as group-III precursors and arsine as group-V precursor. Disilane was used as the dopant precursor to obtain n -type doping. Undoped GaAs wafers (2") with crystal orientation (100), 15° off towards $\langle 111 \rangle$ were used as substrates. A typical sample consisted of a 15 nm Si-doped AlAs and a $5 \mu\text{m}$ undoped $\text{Al}_x\text{Ga}_{1-x}\text{As}$ overlayer. A growth series with nominal aluminum fractions of $x = 0, 0.3$, and 0.5 was produced ($\text{Al}_{0.0}\text{Ga}_{1.0}\text{As}$, $\text{Al}_{0.297}\text{Ga}_{0.703}\text{As}$, and $\text{Al}_{0.508}\text{Ga}_{0.492}\text{As}$). An additional sample with $x \approx 0.5$ ($\text{Al}_{0.489}\text{Ga}_{0.511}\text{As}$) was grown on a substrate 2° off towards $\langle 110 \rangle$. The stoichiometry, used to identify the samples, was obtained from high-resolution x-ray diffraction rocking curve measurement (HRXRD) immediately after growth. An epitaxial lift-off process⁶ was applied to separate the $\text{Al}_x\text{Ga}_{1-x}\text{As}$ layer from the substrate by selectively etching the intermediate Si-doped AlAs layer with a hydrogen fluoride (HF) solution.⁷ The $\text{Al}_x\text{Ga}_{1-x}\text{As}$ thin films (mg quantities, $\sim 10^{18}$ spins) were then powderized to typical grain sizes of a few micrometer and transferred to quartz tubes for NMR measurements.

Figure 2(a) shows the ^{75}As ($I = 3/2$) spectra of $\text{Al}_{0.297}\text{Ga}_{0.703}\text{As}$ and $\text{Al}_{0.489}\text{Ga}_{0.511}\text{As}$ recorded at a Larmor frequency of $\nu_0 = 51.24 \text{ MHz}$ (7.02 T field) on a Infinity-plus spectrometer (Varian Inc.) using a home-built static probe assembly. Two peaks can be observed in both spectra. A comparison with AlAs (Alfa Aesar, 99.9%) and GaAs (semi-insulating, Wafer Technology LTD) powder samples in Fig. 2(b) suggests that the lines correspond to the As configurations with equal nearest neighbors, namely $\text{As}[\text{Al}_4]$ and $\text{As}[\text{Ga}_4]$, with a chemical shift difference of $\sim 180 \text{ ppm}$. The absence of a signal from the remaining $^{75}\text{As}[\text{Al}_n\text{Ga}_{4-n}]$ ($n = 1, 2, 3$) sites with a mixed first coordination shell can be explained by the large second-order quadrupole broadening of their central transition, while the quadrupole coupling is

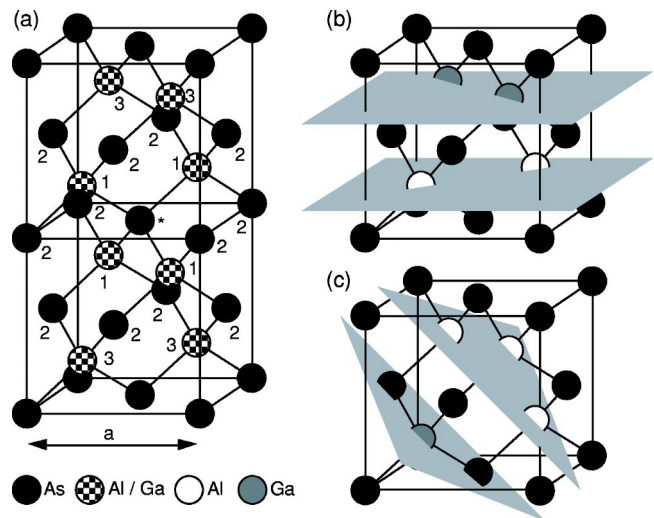


FIG. 1. (a) Two unit cells of the fcc $\text{Al}_x\text{Ga}_{1-x}\text{As}$ lattice. Filled spheres indicate anion (As) and checked spheres cation sites (Al, Ga). The neighboring atoms of the central As (asterisk) are numbered according to their coordination sphere. Coordination numbers and distances are 4 and 2.45 \AA for the first sphere (occupied by either Al or Ga), 12 and 4.00 \AA for the second sphere (As), as well as 12 and 4.69 \AA for the third sphere (Al, Ga). The lattice constant is given by $a_x = 5.66140 + 0.00809x \text{ \AA}$ (Ref. 8). (b) Fully CuAu ordered $\text{Al}_{0.5}\text{Ga}_{0.5}\text{As}$ with alternating AlAs and GaAs planes along the (001) direction. (c) CuPt ordered lattice where planes extend along (111).

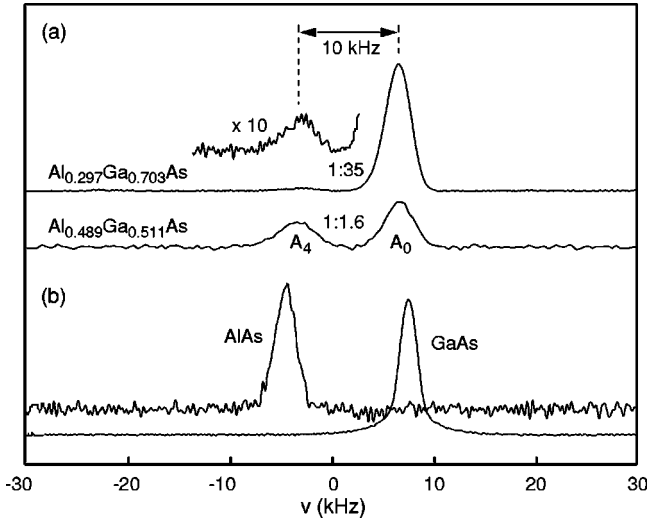


FIG. 2. Single-pulse ^{75}As spectra of $\text{Al}_{0.297}\text{Ga}_{0.703}\text{As}$ (540 k transients) and $\text{Al}_{0.489}\text{Ga}_{0.511}\text{As}$ (62 k transients). All measurements were performed under ambient conditions. Only the central ($\pm[\frac{1}{2} \leftrightarrow -\frac{1}{2}]$) transition is visible. The ratio of the integrated peak areas ($A_0:A_4$) is 35:1 and 1.6:1, respectively. (b) Reference spectra of AlAs and GaAs. The lines are shifted by about -1 kHz and $+1$ kHz with respect to the $\text{As}[\text{Al}_4]$ and $\text{As}[\text{Ga}_4]$ resonances in the mixed samples.

much weaker for the $\text{As}[\text{Al}_4]$ and $\text{As}[\text{Ga}_4]$ sites which are tetrahedral within the first coordination sphere. Our interpretation is corroborated by a quantitative study of ^{75}As signal intensities as well as echo experiments (*vide infra*). The ^{27}Al ($I=5/2$), ^{69}Ga , and ^{71}Ga ($I=3/2$) NMR spectra of these samples were also recorded. All of them showed a single Gaussian peak with a linewidth of 2.7 kHz (^{27}Al , ^{69}Ga) and 2.9–3.3 kHz (^{71}Ga), respectively. Furthermore, it was verified by comparison with the GaAs reference that the observed resonance line intensities for ^{69}Ga and ^{71}Ga contain the signal from all spins in the sample. This absence of broad Ga lines is consistent with the fcc lattice model of Fig. 1(a) which places both Al and Ga in a tetrahedral As cage. Further, the presence of a single Ga resonance implies that chemical-shift effects induced by changes in the second coordination sphere are too small to be resolved in our experiment.

The large chemical-shift difference between $^{75}\text{As}[\text{Al}_4]$ and $^{75}\text{As}[\text{Ga}_4]$ enables the extraction of quantitative structural information for the $\text{Al}_x\text{Ga}_{1-x}\text{As}$ samples. The degree of atomic ordering can be characterized by an order parameter S defined as²

$$S = x'_{\text{Al}} + x'_{\text{Ga}} - 1, \quad (1)$$

where x'_{Al} and x'_{Ga} are the fractions of Al and Ga sites that are occupied by the preferred atom. Conversely, a local deviation from the bulk stoichiometry is given by $x'_{\text{Al}} = x \pm S/2$ and $x'_{\text{Ga}} = 1 - x \pm S/2$, where the different sign refers to an enhanced or reduced probability of finding an Al or Ga atom at a certain site. Using this notation, the probability of an

TABLE I. $\text{Al}_{0.489}\text{Ga}_{0.511}\text{As}$ quadrupole coupling parameters and spin-lattice relaxation times (300 K).

	C_{qcc} (kHz)	η	T_1 (s)
^{27}Al	83 ± 7	> 0.96	16.1 ± 0.4
^{71}Ga	310 ± 10	> 0.95	0.77 ± 0.04
^{69}Ga	520 ± 20	> 0.97	0.29 ± 0.01
$^{75}\text{As}[\text{Ga}_4]$	610 ± 20	> 0.97	0.16 ± 0.06
$^{75}\text{As}[\text{Al}_4]$	820 ± 50	> 0.88	0.14 ± 0.08
^{75}As (other)	> 9 MHz		

^aFor spin $I=5/2$ (^{27}Al), $\nu_Q = \frac{3}{20} C_{\text{qcc}}$.

^b $\text{Al}_{0.508}\text{Ga}_{0.492}\text{As}$, solid echo experiment.

$\text{As}[\text{Ga}_4]$ configuration for different types of ordering (i.e., CuAu, CuPt, or clustering) is then given by⁴

$$p_0^{(\text{CuAu})} = 1/2(1-x-S/2)^2(1-x+S/2)^2 + 1/2(1-x+S/2)^2(1-x-S/2)^2, \quad (2)$$

$$p_0^{(\text{CuPt})} = 1/2(1-x-S/2)^3(1-x+S/2) + 1/2(1-x+S/2)^3 \times (1-x-S/2), \quad (3)$$

$$p_0^{(\text{clust})} = x[1-x-S(1-x)]^4 + (1-x)(1-x+Sx)^4, \quad (4)$$

and for the $\text{As}[\text{Al}_4]$ configuration by

$$p_4^{(\text{CuAu})} = 1/2(x+S/2)^2(x-S/2)^2 + 1/2(x-S/2)^2(x+S/2)^2, \quad (5)$$

$$p_4^{(\text{CuPt})} = 1/2(x+S/2)^3(x-S/2) + 1/2(x-S/2)^3(x+S/2), \quad (6)$$

$$p_4^{(\text{clust})} = x[x+S(1-x)]^4 + (1-x)(x-Sx)^4, \quad (7)$$

where the contributions from the Al and Ga rich zones are reflected in the first and second term of each equation (2)–(7), respectively. For $x \neq 0.5$, complete CuAu- or CuPt-type ordering (i.e., $S=1$) cannot be reached, however, it is possible for clustering, where $S=1$ corresponds to phase separation.

Quantitative information on the order parameter S is inferred from the ratio of the $^{75}\text{As}[\text{Al}_4]$ and $^{75}\text{As}[\text{Ga}_4]$ line intensities (p_0/p_4) (Ref. 9) obtained from the spectra shown in Fig. 2(a) as well as from absolute ^{75}As line intensities obtained by comparison with a GaAs reference sample yielding (p_0+p_4). The measurement of (p_0+p_4) was performed by a quantitative analysis of the ^{75}As signal from different $\text{Al}_x\text{Ga}_{1-x}\text{As}$ samples. The single pulse (4.4 μs duration, 37 kHz rf-field strength) spectra were normalized by a scaling factor taking the effective nutation of the two ^{75}As resonances into account for the given rf-field strength. The nutation and possible contributions of the satellite transitions to the signal were calculated using the experimental quadrupole coupling constants of $\text{Al}_{0.489}\text{Ga}_{0.511}\text{As}$ (see Table I).¹⁰ The overall accuracy of the measurements was within $\pm 5\%$, checked by the ^{71}Ga intensities where no configurational features can be detected. The experimental (p_0/p_4) and (p_0+p_4) values for $\text{Al}_{0.297}\text{Ga}_{0.703}\text{As}$ and $\text{Al}_{0.508}\text{Ga}_{0.492}\text{As}$ are

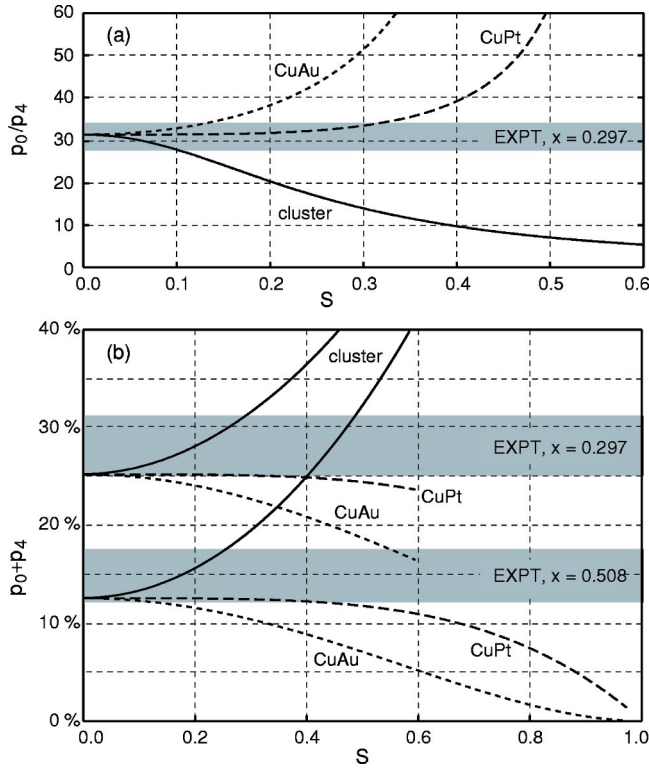


FIG. 3. (a) (p_0/p_4) and (b) (p_4+p_0) vs the order parameter S for CuAu (dotted) and CuPt (dashed) order as well as for clustering (solid line). The experimental results are included by their 95% confidence interval (shaded). They are compatible with $S^{(\text{CuAu})} < 0.14$, $S^{(\text{CuPt})} < 0.32$, $S^{(\text{clust})} < 0.11$ for $\text{Al}_{0.297}\text{Ga}_{0.703}\text{As}$ (a), $S^{(\text{CuAu})} < 0.10$, $S^{(\text{CuPt})} < 0.40$, $S^{(\text{clust})} < 0.30$ for $\text{Al}_{0.297}\text{Ga}_{0.703}\text{As}$ [(b), upper interval] and $S^{(\text{CuAu})} < 0.16$, $S^{(\text{CuPt})} < 0.47$, $S^{(\text{clust})} < 0.26$ for $\text{Al}_{0.508}\text{Ga}_{0.492}\text{As}$ [(b), lower interval].

shown in Figs. 3(a) and 3(b). The results are compatible with the absence of any significant ordering. Upper limits for $S^{(\text{clust})}$ and $S^{(\text{CuAu})}$ are ~ 0.15 using the (p_0/p_4) criterion, or 0.20 and 0.30, respectively, using the (p_0+p_4) criterion. However, for $S^{(\text{CuPt})}$ only strong ordering can be excluded. It is evident that clustering and CuAu ordering have a strong influence on both (p_0/p_4) and (p_0+p_4) and can therefore be well characterized by NMR, while a CuPt-ordered structure requires at least $S > 0.4$ to show significant changes in the NMR spectra.

If no ordering is present, the aluminum fraction x can be inferred from (p_0/p_4) , yielding $x = 0.29 \pm 0.01$ ($\text{Al}_{0.297}\text{Ga}_{0.703}\text{As}$), 0.47 ± 0.01 ($\text{Al}_{0.489}\text{Ga}_{0.511}\text{As}$), and 0.47 ± 0.02 ($\text{Al}_{0.508}\text{Ga}_{0.492}\text{As}$). We attribute the deviations at higher x to a partial relaxation of the thin film material¹¹ where HRXRD measurements tend to overestimate the aluminum fraction.

Additional structural information about the $\text{Al}_x\text{Ga}_{1-x}\text{As}$ thin-film samples is obtained by an analysis of the nuclear quadrupole parameters. The measurements were performed on $\text{Al}_{0.489}\text{Ga}_{0.511}\text{As}$. For all nuclei, the coupling constant $C_{\text{qcc}} = e^2qQ/h$ and asymmetry parameter $\eta = (V_{xx} - V_{yy})/V_{zz}$ (Ref. 12) were measured by nutation NMR.^{13,14} A series of representative nutation spectra for ^{71}Ga is given

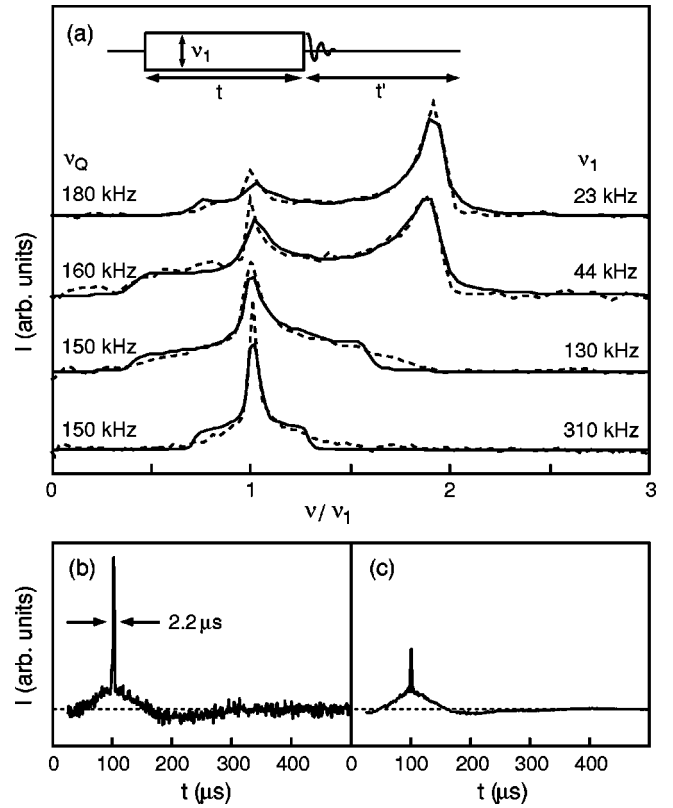


FIG. 4. (a) Nutation spectra of ^{71}Ga in $\text{Al}_{0.489}\text{Ga}_{0.511}\text{As}$ (dotted) obtained using the pulse-timing diagram shown in the figure. The Fourier transform with respect to t at $t' = 0$ is displayed. The Fourier transform with respect to t at $t' = 0$ is displayed. C_{qcc} , η , ν_1 , and a Lorentzian line broadening were used as parameters in the least-squares fits (solid line). The values on the left and right side are the quadrupole frequency ($\nu_Q = \frac{1}{2}C_{\text{qcc}}$ for spin $I = 3/2$) and the rf-field strength ν_1 as obtained from the fits. (b) Solid echo of ^{75}As in $\text{Al}_{0.489}\text{Ga}_{0.511}\text{As}$ as produced by the pulse sequence $(\pi/2)_x - \tau - (\pi/2)_y - (\text{acq})$ with $\tau = 100 \mu\text{s}$. A broad echo from the two resolved peaks and a spike at the exact echo position are observed. The sharp echo peak in the experimental signal is much more intense than the calculated intensity (c) assuming only the two $\text{As}[\text{Al}_4]$ and $\text{As}[\text{Ga}_4]$ resonances (and their satellite transitions) to be present, suggesting that the major contribution to the sharp echo stems from the $n = 1, 2, 3$ central transitions. The spectra are normalized to the intensity of the respective central transition.

in Fig. 4(a). Special attention was paid to B_1 inhomogeneities for rf-field strengths up to 350 kHz (16-turn, 1.3 mm diameter solenoid rf coil). From the scaling behavior of the nutation linewidth vs rf-field strength we estimate the variations in the latter to be less than 7%. Resonance offsets were avoided as far as possible, and included in the simulations if necessary. Recycle delays were set to $5T_1$. The results are summarized in Table I. Four spectra at different rf-field strengths were recorded for each nucleus and fitted individually, providing independent values for C_{qcc} and η . The average value and standard deviation is reported for C_{qcc} while a lower bound is given for η .

Since the quadrupole coupling is induced by the electric-field gradient (EFG) caused by a mixed occupation of the cation sites the C_{qcc} values are best categorized according to the different coordination spheres. First-shell effects are only

observed for ^{75}As in the mixed $\text{As}[\text{Al}_n\text{Ga}_{4-n}]$ ($n=1,2,3$) configuration. Their presence is witnessed in solid echo spectra shown in Fig. 4(b). The sharp echo peak in the experimental signal is much more intense than the calculated intensity assuming only the two $\text{As}[\text{Al}_4]$ and $\text{As}[\text{Ga}_4]$ resonances (and their satellite transitions) to be present. This indicates that the major contribution to the sharp echo peak originates from the strongly broadened $n=1,2,3$ central transitions. A similar experiment performed under identical conditions for ^{69}Ga (with a slightly smaller quadrupole coupling constant) shows a much lower intensity for the sharp echo feature which is in this case produced by the satellite transitions only, as was confirmed by simulations (not shown). A lower bound of the C_{qcc} can be estimated from the echo width of $\Delta\tau \approx 2.2 \mu\text{s}$ implying a linewidth for the central transition of at least $\Delta\nu_{\pm[1/2 \leftrightarrow -1/2]} \geq 0.883/\Delta\tau \approx 400 \text{ kHz}$. Using the approximation $\nu_Q^2 > \Delta\nu_{\pm[1/2 \leftrightarrow -1/2]}\nu_0$ we can estimate $C_{\text{qcc}} = 2\nu_Q > 9 \text{ MHz}$. It has to be remarked that the echo width is rather limited by the rf pulse strength ($\nu_1 \approx 230 \text{ kHz}$) than the intrinsic linewidth of the $\text{As}[\text{Al}_n\text{Ga}_{4-n}]$ ($n=1,2,3$) resonances.

For the sites with a symmetric first coordination sphere, the dominant influence on the quadrupole interaction stems from the second (Al,Ga as central atom) or third (central As) nearest neighbors. In a disordered structure, many arrangements of Al and Ga atoms are possible, all of them potentially leading to a different coupling strength. It has been demonstrated that a close to Gaussian distribution of coupling constants and an asymmetry parameter distribution dominated by values >0.5 can be expected for related disordered systems, with a vanishing probability of symmetric ($C_{\text{qcc}}=0$ and $\eta=0$) contributions.^{15,16} Contrarily, if ordering is present, a substantial tetrahedrally symmetric fraction of Al (and Ga) emerges [see Figs. 1(b) and 1(c)] (neglecting

effects from 4th and outer spheres). This would result in a strong $\nu=\nu_1$ component in the nutation spectra and a lowering in the η values. Both is, however, not observed in our experiments. The effect of ordering on the nutation spectra can be quantified using a bimodal approach, where a $C_{\text{qcc}}=0$ fraction is added to a spectrum with a fixed, nonzero C_{qcc} . Varying the added fraction and the magnitude of the fixed C_{qcc} , fitting errors become intolerable if the symmetric fraction exceeds $\sim 8\%$, which corresponds to $S > 0.5$ for all investigated types of ordering.

Further insight in local structure and (dis)order might be obtained by comparing the quadrupolar parameters, and their possible distributions, as a function of composition for the different nuclei in the sample. Their interpretation calls for *ab initio* calculations of the EFG tensors, however, which is beyond the scope of the present contribution.

In conclusion, we have presented a structural NMR study on $\text{Al}_x\text{Ga}_{1-x}\text{As}$ thin films. The locally symmetric $\text{As}[\text{Al}_4]$ and $\text{As}[\text{Ga}_4]$ sites are directly resolved in the ^{75}As spectrum, while the other resonances from $\text{As}[\text{Al}_n\text{Ga}_{4-n}]$ ($n=1,2,3$), although undetectable in the direct spectrum due to large second-order quadrupolar broadenings, can be tracked by their solid echo. The intensity of the $\text{As}[\text{Al}_4]$ and $\text{As}[\text{Ga}_4]$ lines are connected to configurational probabilities predicted for different types of ordering, i.e., CuAu- and CuPt-type ordering as well as clustering. Within this framework we find that all our $\text{Al}_x\text{Ga}_{1-x}\text{As}$ samples are compatible with a completely random Al, Ga distribution. In addition, a quantitative analysis of the nuclear quadrupole coupling yields $\eta \approx 1$ for all investigated nuclei, indicating that no axial symmetry of the EFG tensor is present. The measured quadrupole coupling constants agree with the model of a number of random cation configurations in the second coordination as opposed to a strongly ordered structure where a dominant fraction with $C_{\text{qcc}}=0$ would be expected.

*Electronic address: beme@ethz.ch

†Electronic address: arno.kentgens@nmr.kun.nl

¹P.M. Petroff, A.Y. Cho, F.K. Reinhart, A.C. Gossard, and W. Wiegmann, *Phys. Rev. Lett.* **48**, 170 (1982).

²T.S. Kuan, T.F. Kuech, W.I. Wang, and E.L. Wilkie, *Phys. Rev. Lett.* **54**, 201 (1985).

³G.B. Stringfellow and G.S. Chen, *J. Vac. Sci. Technol. B* **9**, 2182 (1991).

⁴R. Tycko, G. Dabbagh, S.R. Kurtz, and J.P. Goral, *Phys. Rev. B* **45**, 13 452 (1992).

⁵A.J. Heinrich, M. Wenderoth, K.J. Engel, T.C.G. Reusch, K. Saathoff, and R.G. Ulbrich, *Phys. Rev. B* **59**, 10 296 (1999).

⁶Eli Yablonowitch, T. Gmitter, J.P. Harbison, and R. Bhat, *Appl. Phys. Lett.* **51**, 2222 (1987).

⁷M.M.A.J. Voncken, J.J. Schermer, G.J. Bauhuis, P. Mulder, and P.K. Larsen, *Appl. Phys. A* (to be published).

⁸N.S. Takahashi, in *EMIS Datareviews Series: Properties of Aluminium Gallium Arsenide*, edited by S. Adachi (INSPEC, London, 1993), Vol. 7, p. 3.

⁹When calculating p_0/p_4 from A_0/A_4 [Fig. 2(a)] a small correction of $\sim 10\%$ due to the different quadrupole couplings of $\text{As}[\text{Al}_4]$ and $\text{As}[\text{Ga}_4]$ applies (Ref. 10).

¹⁰The signal intensity $A_n^{j,k}$ of nucleus j in sample k with configuration n is proportional to $(m^k/M^k)p_n x^{k,j} I_{\text{scale}}^{j,k}$, where p_n is the configurational probability as introduced in the text, m^k the mass, M^k the molecular weight, and $x^{k,j}$ the stoichiometric fraction of the respective sample and nucleus. The scaling factor $I_{\text{scale}}^{j,k}$ accounts for nutation and different signal contributions of satellite and central transition.

¹¹C. Carter-Coman, R. Bicknell-Tassius, A.S. Brown, and N.M. Jokerst, *Appl. Phys. Lett.* **70**, 1754 (1997).

¹²D. Freude and J. Haase, in *NMR Basis Principles and Progress: Quadrupole Effects in Solid-State Nuclear Magnetic Resonance*, edited by P. Diehl, E. Fluck, H. Günther, R. Kosfeld, and J. Seelig (Springer, Berlin, 1993), Vol. 29.

¹³A. Samoson and E. Lippmaa, *Phys. Rev. B* **28**, 6567 (1983); *Chem. Phys. Lett.* **174**, 309 (1983).

¹⁴A.P.M. Kentgens, J.J.M. Lemmens, F.M.M. Geurts, and W.S. Veeman, *J. Magn. Reson.* (1969-1992) **71**, 62 (1987).

¹⁵A.J. Pustowka, B.D. Sawicka, and J.A. Sawicki, *Phys. Status Solidi B* **57**, 783 (1973).

¹⁶G. Czjzek, J. Fink, F. Götz, H. Schmidt, J.M.D. Coey, J.-P. Rebouillat, and A. Linard, *Phys. Rev. B* **23**, 2513 (1981).